Control Strategies for Grid Connected PWM-VSI Systems

Emre Kantar[1,2,4], S. Nadir Usluer[1,3,5], and Ahmet M. Hava[1,6]

[1]Middle East Technical University, Electrical and Electronics Engineering Department, Çankaya Ankara, Turkey
[2]Microelectronics, Guidance & Electro-Optics Division, ASELSAN INC., Akyurt, Ankara, Turkey
[3]Defense Systems Technologies, ASELSAN INC., Yenimahalle, Ankara, Turkey
[4]emre.kantar@metu.edu.tr [5]nadir.usluer@metu.edu.tr [6]hava@metu.edu.tr

Abstract

This paper evaluates the current control methods for three-phase voltage-source-inverters (VSIs) connected to the grid via LCL-filters. Current feedback methods from both line and converter sides are compared and theoretical analysis is stated. The analysis is based on the existence of a critical resonant frequency dividing the controlling frequency interval into two regions; namely low and high resonant frequency regions. The feedback types and damping methods are evaluated for both low and high resonant frequency regions with regard to resonant and low frequency poles of the system. In the low resonant frequency region, damping of LCL-filter resonance is necessary for line current feedback; while the current controller provides inherent damping when converter current feedback is utilized. Moreover, total harmonic distortion (THD) and power factor performance of the designed system employing either line or converter current feedback is assessed under varying load conditions. Besides, thorough theoretical approaches supported with simulation results are presented.

1. Introduction

Three-phase grid connected pulse-width modulation (PWM) inverters are getting more popular due to enhanced controllability, high efficiency, and reliable performance with long life. The connection to the electric utility is provided through LCL line filters in modern PWM voltage source inverters (VSIs) ensuring a more compact system and better harmonic attenuation compared to the conventional L filters. However, the presence of resonant frequency (f_{res}) inherent to LCL-filters may result in amplification of undesired harmonics causing high frequency oscillations in the current controllers. In the literature, this phenomenon is dealt with the employment of various resonance damping methods such as passive damping (PD) provided with resistors connected in several ways to the LCL-filter [1], [3]; active damping (AD) supplied with the modification of the current control structure using filter capacitor current [2]-[5], or capacitor voltage [2], or filter based techniques [4] or complex state observers. However, most of the papers in the literature neither regard the location of f_{res} of filter nor examine both of the line-side current feedback (LF) and converter-side current feedback (CF) techniques at the same time. Nonetheless, the analysis on the control strategies for a PWM-VSI connected to the grid via an LCL-filter requires a deeper approach, handling the resonance problem for different f_{res}. In [5], the regions of AD are considered; whereas, in [1] LF and CF are compared regarding the control actions. Nevertheless, none of them present a clear comparison on different feedback methods concerning both high and low f_{res} regions. All in all, literature lacks a complete design study comparing LF and CF methods by regarding f_{res} at low and high frequency regions. This paper also considers the dynamic and step responses of the system, FFT analysis of the line side currents, THD and power factor (PF) performance of the system under varying loads to state a complete comparison between LF and CF including the selection of f_{res}. The main objective of this paper is to provide the optimum current control technique with regard to the power rating of the system.

Firstly, the system to be studied is described and mathematical model is depicted in Section 2. Then, controller design and feedback types are explained in Section 3. Regions of control for current controllers are analyzed in Section 3.3. The validation of theoretical studies via simulations is achieved in Section 4, and the conclusions are given at the very end.

2. Modeling and Description of the System

Fig. 1 demonstrates a three-phase VSI connected to the grid via an LCL-filter. The current feedback method for the closed loop controller in Fig. 1 is LF. The ideal LCL-filter consumes only reactive power; nevertheless, the components in real life have resistive parts. However, the winding resistance and core loss of line-side and converter-side filter inductors (L_g, L_c) and ESRs of filter capacitors (C_f) are neglected in controller design phase to provide a worst case undamped situation.

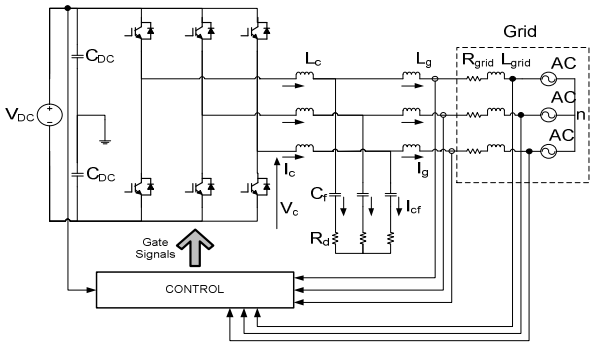

Fig.1. Grid connected 3-phase VSI with line current feedback

The transfer function of LCL-filter between the line-side current (I_g) and the converter output voltage (V_c) is defined in (1). (1) implies the situation when LF is employed as the current control feedback variable. The relation between I_g and the filter capacitor current (I_{cf}) is defined in (2) using L_g and C_f.

$$Y_{LCL}(s) = G_p(s) = \frac{I_g(s)}{V_c(s)} = \frac{1}{s^3 C_f L_c L_g + s(L_c + L_g)} \qquad (1)$$

$$\frac{I_{cf}(s)}{I_g(s)} = s^2 C_f L_g \qquad (2)$$

This paper contains the examination of both LF and CF techniques concerning the damping necessities of each method with regard to the region of f_{res}. Each damping method has its own characteristic features which may be appealing in terms of design simplicity or cost. The power rating is also an important constraint since high power applications are generally not suitable for AD due to very limited switching frequencies around a few kHz [10]. Hence, detailed analysis is yet to be presented in the following sections.

3. Controller Design

In this paper, stabilization is not regarded as the only aim of the controller design procedure, damping extent of the resonance poles are also investigated and correlated with high frequency oscillations occurring at the transient periods. Apart from resonance poles, low frequency poles (dominant poles) of the system are also considered to comment on overshoot percentages of the dynamic responses presented by means of MATLAB and SIMPLORER outputs.

3.1 Controller Modeling

Fig. 2 shows the current controller structure of a three-phase VSI. Either I_g or converter-side current (I_c) can be set as the main feedback variable noting that the LCL-filter transfer function differs in each case. The current controller regulates the active and reactive components of the main feedback variable in synchronous reference frame which is locked directly to the grid voltage vector. The phase angle of line voltages are determined using phase-locked loop (PLL) algorithm stated in [7].

The controlling action is executed at a sampling frequency (f_{samp}) which is twice of the switching frequency f_{sw}. Therefore, the preferred sampling mode is double update sampling mode as in [2] and $T_{samp} = T_{sw}/2$ throughout this paper. Besides, the proportional gain constant K_p and the integral time constant T_I of the PI current controller are selected with the approximation that LCL-filter converges to a simple L filter at low frequencies [2] and tuned according to symmetrical optimum [8] and defined in (3) and (4) respectively as shown below.

$$K_p = \frac{L_c+L_g}{3T_c} \qquad (3) \qquad T_I = 9T_c \qquad (4)$$

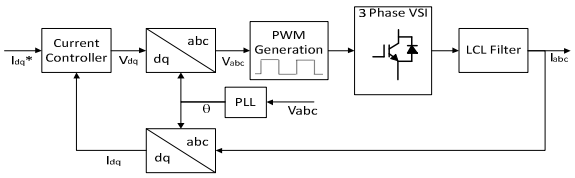

Fig.2. Current control structure

3.2 Current Feedback Methods

In Fig. 3, the system of LCL-filter plant together with PI current controller is fed back with i_g. Resulting open-loop transfer function is shown in (5). Note that there is no s^3 damping term in the denominator making the system undamped. Therefore, instability in the controller due to high frequency oscillations is inevitable.

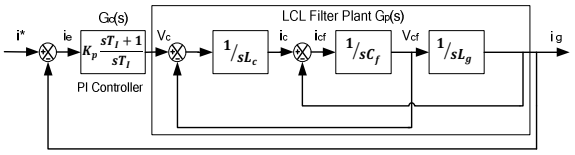

Fig.3. Block diagram of LF

$$\frac{I_g(s)}{I_e(s)} = G_c(s)G_p(s) = \frac{K_p(s+1/T_I)}{s^4 C_f L_c L_g + s^2(L_c+L_g)} \qquad (5)$$

When AD is utilized by using i_{cf} as in Fig. 4, the damping term s^3 appears in the denominator of the open-loop transfer function in (6) to provide damping.

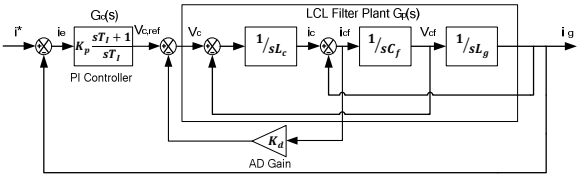

Fig.4. Block diagram of LF with AD

$$\frac{I_g(s)}{V_{c,ref}(s)} = \frac{1}{s^3 C_f L_c L_g + s^2 K_d C_f L_g + s(L_c+L_g)}$$

$$\frac{I_g(s)}{I_e(s)} = \frac{K_p(s+1/T_I)}{s^4 C_f L_c L_g + s^3 K_d C_f L_g + s^2(L_c+L_g)} \qquad (6)$$

On the other hand, once CF is employed, the control block diagram should be modified by changing the feedback variable from i_g to i_c on the schematic. With the use of CF, there will be an additional damping effect inherent to CF type [4]. However, to obtain the resulting open-loop transfer function, some arrangements should be made on the diagram since the feedback variable is tapped from the middle of the loop path. Hence, this impact is modeled as in Fig. 5 by reflecting the relationship between i_g and i_{cf} in (2). Since i_c is the summation of i_g and i_{cf}, CF contains extra i_{cf} information unlike LF. Thereby, block diagram of CF case is depicted as if LF is employed and the difference in between is reflected by subtracting i_{cf} from error current (i_e) to represent the equivalent block diagram of CF [4].

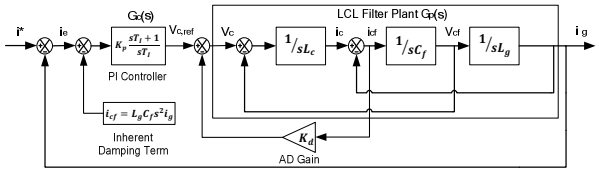

Fig.5. Block diagram of CF with AD (Set K_d=0 for the case without AD)

$$\frac{I_g(s)}{I_e(s)} = \frac{K_p(s+1/T_I)}{s^4 C_f L_c L_g + s^3 K_p C_f L_g + s^2(K_p C_f L_g/T_I + L_c + L_g)} \qquad (7)$$

$$\frac{I_g(s)}{I_e(s)} = \frac{K_p(s+1/T_I)}{s^4 C_f L_c L_g + s^3(K_p+K_d) C_f L_g + s^2(K_p C_f L_g/T_I + L_c + L_g)} \qquad (8)$$

Fig. 5 also presents the AD case in CF method just as depicted in Fig. 4. The open-loop transfer functions without AD and with AD are shown in (7) and (8), respectively. The extent of damping introduced can be tuned by adjusting K_p and proportional AD gain constant K_d to size the damping term coefficient (s^3) in the denominators. Designation methods of K_d have been presented in literature [4], [5]. In this paper, the approach in [4] is adopted to find optimum K_d value. K_d value in the closed-loop transfer functions is varied by means of mathematical tools and optimum value is obtained.

3.3. Regions of Control

The parameters of the system studied in this paper are given in Table 1. They are acquired from presented design procedure in [9]. C_f value is left for the analysis on the forthcoming sections. Modulation index, M_i convention is adopted as in [6].

Table 1. System Parameters

f_{sw}	Switching Frequency	5 kHz	V_{DC}	DC Bus Voltage	750 V
f_g	Grid Frequency	50 Hz	P_{rated}	Rated Power	250 kW
f_{samp}	Sampling Frequency	10 kHz	M_i	Modulation Index	0.679
V_g	Grid Phase Voltage	230 V_{rms}	L_c	Converter Side Inductor	243µH

In this phase, a new variable called critical LCL-filter resonance frequency (ω_{crit}) should be introduced which splits the controlling frequency interval into two regions namely low and high resonant frequency regions [5]. Then, these regions will be examined by regarding the necessity of damping methods in the forthcoming sections. ω_{crit} for the designed VSI can be calculated using (9).

$$\omega_{crit} = \pi/3T_{samp} \tag{9}$$

Fixing the problems caused by inadequate damping is as crucial as the stabilization of an LCL-filter current regulator. Therefore, stabilization is not the only aim of the controller design procedure; sufficient damping must be provided to damp high frequency oscillations caused by resonant poles. Note that f_{res} should not get close to f_{crit} since there is an uncertain and probably unstable region of operation at or near to f_{crit} [5]. Throughout this paper, f_{samp} is kept constant and the variation of f_{res} is investigated with both CF and LF. This analysis requires two sets of LCL parameters: one below f_{crit}, and the other above f_{crit} as listed in Table 2. The inductors are kept constant while C_f is changed to shift f_{res} between low and high f_{res} regions.

Table 2. Selection of C_f below and above f_{crit}

Reactive power absorption ratio (x)	C_f	f_{res}
0.029	$145\mu F$	1.19 kHz
0.015	$74.7\mu F$	1.67 kHz (f_{crit})
0.003	$14.5\mu F$	3.76 kHz
0.002	$10\mu F$	4.57 kHz

3.3.1. LCL Resonance frequency above ω_{crit}

LCL-filter resonant frequency, ω_{res} selected above ω_{crit} is mentioned to belong in high f_{res} region in literature [5]. In this region, employment of AD methods does not promote stability performance and simply LF is sufficient to ensure stability with the usage of conventional current regulators. I_c can also be adopted as the main feedback variable (CF) and a stable system can be obtained without use of AD methods as well. However, the utilization of AD by using I_{cf} may flourish the damping capability of the system and improve the harmonic and ripple performances for both feedback techniques at high f_{res} region.

3.3.2. LCL Resonance frequency below ω_{crit}

LCL-filter resonant frequency, ω_{res} selected below ω_{crit} is mentioned to belong in low f_{res} region in literature [5]. In this region, only CF is sufficient for stable control and utilization of AD provides no enhancement in stability performance. In addition, it does not make any influence on the damping performance of the filter. However, if LF is employed, then AD is essential for stability [2]-[5].

Commercial inverters use CF to sense any kinds of over-current immediately. CF provides inherent damping characteristics due to the presence of I_{cf} information in I_c [4]. Note that the selection of ω_{res} below ω_{crit} can only be feasible in low and medium power applications due to sufficient controller bandwidth of the systems. However, selection of f_{res} requires a different approach for high power systems since f_{sw} is very limited in these applications confining the controller bandwidth to a very narrow region [10]. In stability analysis, the distance between ω_{res} and zero dB gain crossover frequency (ω_c) in the magnitude response of the closed loop system plays the key role to achieve an adequate phase margin. For this reason, ω_c must be fixed sufficiently below ω_{res} regardless of damping extent and technique [9]. Setting $\omega_c \approx 0.3\omega_{res}$ not only succeeds an adequate phase margin (50°) but also avoids the rapid phase transition securely [4], [5], [9]. Besides, K_p value is also vital on succeeding sufficient phase margin; excessive K_p amounts degrade the phase margin. All in all, the analysis shown in Section 4 provides a thorough visual understanding of each controlling method in the regions below and above ω_{crit}.

4. Simulation Studies

In this section, the system presented in Table 1 will be simulated for both low f_{res} and high f_{res} cases by changing C_f value as depicted in Table 2. Additionally, these comparisons will be held for CF and LF techniques. Thus, four distinct cases will be compared and contrasted.

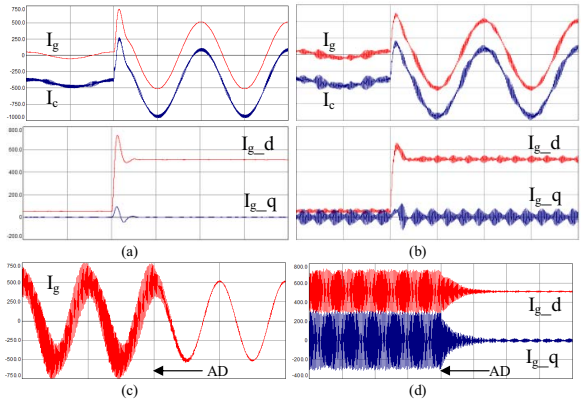

Fig.6. Simulation results of LCL-filter-based inverter using **(a)** LF with AD (low f_{res}, C_f=145µF) **(b)** LF w/o AD (high f_{res}, C_f=10µF) **(c), (d)** LF (high f_{res}, C_f=14.5µF)

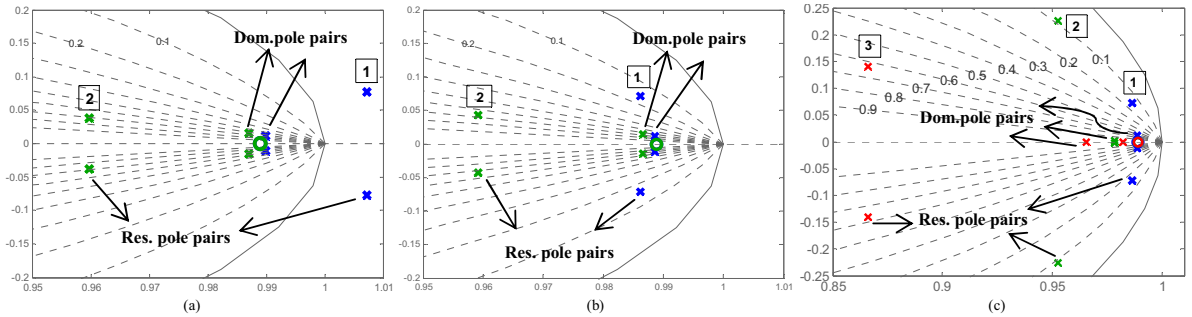

Fig.7. Pole & zero maps of the closed-loop system for **(a)** 1- LF w/o AD (high f_{res}, C_f=10μF), 2- LF with AD (low f_{res}) **(b)** 1- CF w/o AD (low f_{res}), 2- LF with AD (low f_{res}) **(c)** 1- CF w/o AD (low f_{res}), 2- CF w/o AD (high f_{res}), 3- CF with AD (high f_{res})

In Fig. 6 (a) and (b), I_g and I_c utilizing LF are shown for C_f=145μF (low f_{res}) and C_f=10μF (high f_{res}), respectively. I_g in dq-frame synchronous to grid frequency is also depicted by I_{g_d} and I_{g_q}. Filtering performance of the LCL-filter is deteriorated at high f_{res} case and LCL-filter has almost converged to an L filter and the benefits provided by LCL-filter have been abandoned. For the low f_{res} case, the system is stable and damped sufficiently; however, the overshoot at the transition from light load to full load is higher than the high f_{res} case.

In Fig. 7 (a), resonant pole pair at 4.57 kHz (high f_{res} case) depicted with 1 is outside the unit circle. However, phase reversal caused by this pair is ineffective to cause oscillations since ω_c is (3142 rad/sec acquired via MATLAB) very far from ω_{res} (28714 rad/sec). Therefore, it can be deduced that system response is determined by the dominant poles inside the unit circle (low frequency poles) and stability of the system is influenced by the damping ratio (ζ) of the resonant poles. On the other hand, stability has been reached by employing AD for low f_{res} case and resonant poles are damped sufficiently as shown with 2 in Fig. 7 (a). However, ζ of the dominant pole pair is less in 2 than in 1 in Fig. 7 (a); thus, the overshoot of the dynamic response is higher in low f_{res} case compared to high f_{res} case as mentioned in the comments of Fig. 6.

When C_f is opted to be 14.5μF (still high f_{res} case), PWM switching pattern excites the harmonics at f_{res} to very large magnitudes as can be seen in the FFT analysis of I_g in Fig. 8 (a). The distorted I_g, I_{g_d} and I_{g_q} waveforms due to the very large resonant harmonic component are also demonstrated in Fig. 6 (c) and (d), respectively. In this case, AD works quite good and the magnitude of the resonant harmonic as well as its side-band components are mitigated to very low percentages (Fig. 8 (b)). Conversely, when C_f =10μF, f_{res} (4.57 kHz) is pushed further to the edge of the controller bandwidth and the system barely suffers from the resonant effect. However, due to very low filter capacitance; the LCL-filter behaves as L-filter. Thus, employment of AD gives no positive contribution to suppress resonant harmonics any more as shown in Fig. 8 (c) and (d).

CF without additional damping is also evaluated for low and high f_{res} cases and resulting waveforms are depicted in Fig. 10 (a) and (b). I_g, I_c, I_{g_d} and I_{g_q} are shown for C_f=145μF (low f_{res}) and C_f =14.5μF (high f_{res}). The filtering performance of the LCL-filter employing CF is poor for high f_{res} case since large resonant harmonics are present at 3.76 kHz as in Fig.9 (a) and (b). Besides, when C_f is selected as 10μF resonant harmonics increased further from 1.5% to 7% of the rated I_g as shown in Fig. 9 (c). This distortion effect can also be recognized in Fig. 10 (c). AD is employed at the instant depicted by the arrows on Fig. 10 (c) and (d). Nevertheless, it has shown only minor improvements on THD (%) as in Fig. 9 (a) and (d) even if the modulation waveform and I_{g_d} in Fig. 10 (d) are cleared.

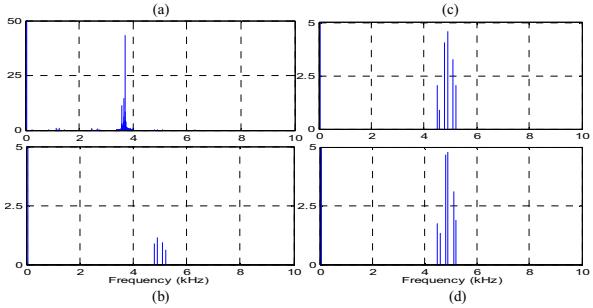

Fig.8. I_g harmonics (%) with LF method for **(a)** C_f=14.5μF **(b)** C_f=14.5μF (AD) **(c)** C_f=10μF **(d)** C_f=10μF (AD)

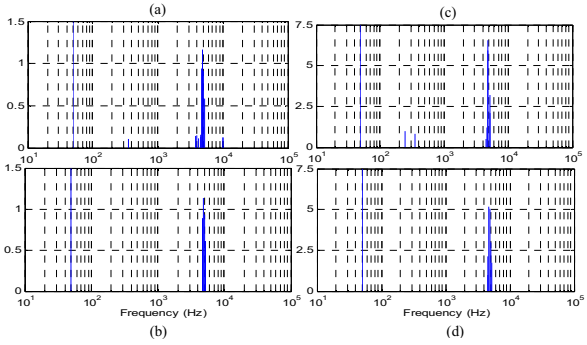

Fig.9. I_g harmonics (%) with CF method for **(a)** C_f=14.5μF **(b)** C_f=14.5μF (AD) **(c)** C_f=10μF **(d)** C_f=10μF (AD)

In the light of above analysis, in high f_{res} case f_{res} should be set as high as possible in the available controller frequency bandwidth to achieve maximum damping of resonant harmonics when LF is employed. Conversely, f_{res} should be selected as close as possible to f_{crit} to succeed the maximum harmonic attenuation when CF is utilized. However, it is suggested that whatever the current feedback type is, f_{res} should be selected in the low f_{res} region in order to maximize the performance of AD as well as the attenuation of LCL-filter. Relying on the inherent damping characteristics of the LCL-filters is not reliable and not practical since any degradation in filter elements may cause loss of stability [4]. Hereafter, the performance analysis of the system employing LF with AD and CF without additional damping in low f_{res} region has been conducted.

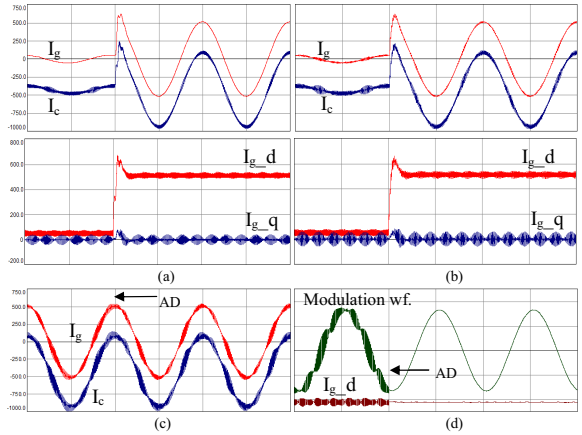

Fig.10. Simulation results of LCL-filter-based inverter using **(a)** CF w/o AD (low f_{res}) **(b)** CF w/o AD (high f_{res}, C_f=14.5μF) **(c)** CF with AD (high f_{res}, C_f=10 μF) **(d)** Modulation wf. & I_{g_d}

In Fig. 7 (b), 2 represents the location of the poles of the system using LF with AD; whereas, 1 denotes the position of the poles of the system using only CF for C_f=145μF (low f_{res}). As can be realized in Fig. 7 (b), ζ of the resonant poles in 2 seems quite satisfactory (ζ=0.7) rather than the poles in 1. Therefore, the dynamic response of 1 is expected to contain high frequency oscillations caused by under-damped resonant poles unlike the dynamic response of 2. Accordingly, In Fig. 10 (a), there are high frequency oscillations in transient period; whereas, there is not any present in Fig. 6 (a). Additionally, in Fig. 11 (a), the step response of 1 contains high frequency oscillations as expected. However, the dominant poles of 1 in Fig. 7 (b) are damped more than the poles in 2 bringing out the overshoot of the dynamic response in 2 become higher than 1. The corresponding outcomes can be recognized by comparing the overshoots of the dynamic responses of I_g waveforms in Fig. 6 (a) and in Fig. 10 (a) (scale is the same) as well as the step responses of 1 and 2 in Fig. 11 (a). Moreover, three cases are compared in Fig.7 (c): low f_{res} without AD, high f_{res} without AD, and high f_{res} with AD. In Fig. 7 (c), the dominant poles of 3 are the most damped pole pairs yielding the least overshoot as can be seen in Fig. 11 (b). Similarly, the dominant poles of 1 are the least damped poles providing the highest overshoot as depicted in Fig. 11 (b). In addition, the resonant poles in case 2 are less damped than the poles in case 1 (Fig. 7 (c)), thus high frequency oscillations are present in Fig. 10 (b) unlike Fig. 10 (a). Consequently, step response in case 2 has high frequency oscillations dissimilar to case 1 in Fig. 11 (b).

Despite little improvements on THD performances with the introduction of AD in CF method at high f_{res} case (Fig. 7 (c)-case 3), the dominant poles become more damped and provide a better dynamic response influence of which can be seen in Fig. 11 (b).

In Fig. 12, FFT analysis shows that LF performed slightly better than CF in THD aspect for all load conditions owing to the effect of the employment of AD in LF case; whereas, in CF only inherent damping characteristics of the LCL-filter are used. Besides, as load percentage increases I_g tends to contain fewer harmonics. Furthermore, Fig. 12 shows that LF is favorable to CF in achieving unity PF since LF directly monitors the currents injected into the grid. The deviation of the PF from unity with the change of load becomes greater as the load percentage decreases.

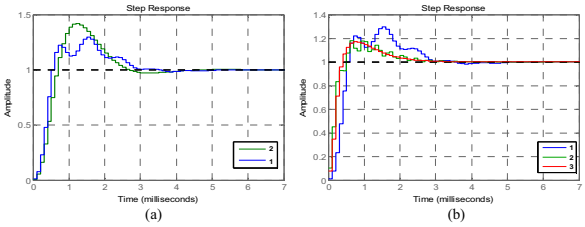

Fig.11. Step response of the system **(a)** 1- CF w/o AD (low f_{res}), 2- LF with AD (low f_{res}) **(b)** 1- CF w/o AD (low f_{res}), 2- CF w/o AD (high f_{res}), 3- CF with AD (high f_{res})

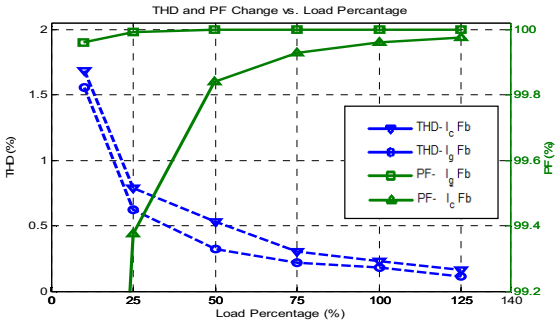

Fig.12. THD and PF change vs. load for CF and LF methods

5. Conclusions

This paper has presented a thorough current control analysis for the grid connected PWM-VSI systems with LCL-filter. The regions of operation of current controller have been divided into two main regions namely; low f_{res} region and high f_{res} region which are separated by f_{crit} at which the stabilization of the current controller is impossible. The controlling action has been examined by utilizing each of the LF and CF for the defined regions of operation. Furthermore, theoretical approaches are proven with elaborated simulation analyses and supported with pole-zero maps, FFT analysis of the produced line current and step responses of the system under changing conditions. The variation of THD (%) and PF under varying loads has also been presented for each current feedback type. For future investigations, the approach obtained in this paper will be implemented on different VSI topologies.

6. References

[1] M. Liserre, F. Blaabjerg, and S. Hansen, "Design and control of an LCL-filter-based three-phase active rectifier, "IEEE. Trans. Ind. Applications, vol. 41, pp.1281-1291, 2005.

[2] J. Dannehl, F.W. Fuchs, S. Hansen, and P.B. Thogersen, "Investigation of Active Damping Approaches for PI-Based Current Control of Grid-Connected Pulse Width Modulation Converters with LCL Filters," IEEE. Trans. Industrial Applications, vol. 46, pp. 1509-1517, 2010.

[3] B.G. Cho, S.K. Sul, "LCL Filter Design for Grid-connected Voltage-source Converters in High Power Systems," IEEE. Trans. Industrial Applications, pp. 1548 – 1555, 2012.

[4] Y. Tang, P. C. Loh, P. Wang, F. H. Choo and F. Gao, "Exploring inherent damping characteristics of LCL-filters for three-phase grid-connected voltage source inverters," IEEE Trans. Power Electron., vol. 27, no. 3, pp. 1433-1443, Mar. 2012.

[5] S. G. Parker, B. P. McGrath, and D. G. Holmes, "Regions of Active Damping Control for LCL Filters" IEEE Trans. Ind. Applicat., 2012-IPCC-463

[6] A. M. Hava, R. J. Kerkman, and T. A. Lipo, "Simple analytical and graphical methods for carrier-based PWM-VSI drives," IEEE Trans. Power Electron., vol. 14, no. 1, pp. 49–61, Jan. 1999.

[7] V. Kaura and V. Blasko, "Operation of a phase locked loop system under distorted utility conditions," in Proc. IEEE 11th Annu. Applied Power Electronics Conf. Expo., Mar. 3–7, 1996, vol. 2, pp. 703–708

[8] D. Schröder, Elektrische Antriebe 2, Regelung von Antriebssystemen, 2nd ed. Berlin, Germany: Springer-Verlag, 2001.

[9] E. Kantar, S. N. Usluer, and A. M. Hava, "Design and Performance Analysis of a Grid Connected PWM-VSI System," submitted to ELECO 2013.

[10] S. N. Usluer, E. Kantar, and A. M. Hava, "Evaluation of PWM-VSI Systems Connected to the Grid through LCL Filters," presented at YEKSEM, 2013.